

# Structure and magnetic behaviour of $[\{\text{Mn}_2(3\text{-Et},4\text{-Mepy})_6(\mu_{1,1}\text{-N}_3)_2(\mu_{1,3}\text{-N}_3)\}_n][\text{PF}_6]_n$ and $[\{\text{Mn}_2(3\text{-ampy})_4(\mu_{1,1}\text{-N}_3)_2(\mu_{1,3}\text{-N}_3)(\text{N}_3)(\text{H}_2\text{O})\cdot 4\text{H}_2\text{O}\}_n]$ , two alternating ferro–antiferromagnetic one-dimensional compounds

Morsy Abu Youssef,<sup>a</sup> Albert Escuer,<sup>b</sup> Mohamed A. S. Goher,<sup>c</sup> Franz A. Mautner<sup>a</sup> and Ramon Vicente<sup>\*b</sup>

<sup>a</sup> Institut für Physikalische und Theoretische Chemie, Technische Universität Graz, A-8010 Graz, Austria

<sup>b</sup> Departament de Química Inorgànica, Universitat de Barcelona, Diagonal 647, 08028 Barcelona, Spain

<sup>c</sup> Department of Chemistry, Faculty of Science, Alexandria University, Alexandria 21321, Egypt

Received 29th September 1999, Accepted 19th November 1999

Two new monodimensional compounds,  $[\{\text{Mn}_2(3\text{-Et},4\text{-Mepy})_6(\mu_{1,1}\text{-N}_3)_2(\mu_{1,3}\text{-N}_3)\}_n][\text{PF}_6]_n$  **1** and  $[\{\text{Mn}_2(3\text{-ampy})_4(\mu_{1,1}\text{-N}_3)_2(\mu_{1,3}\text{-N}_3)(\text{N}_3)(\text{H}_2\text{O})\cdot 4\text{H}_2\text{O}\}_n]$  **2** in which 3-Et,4-Mepy = 3-ethyl-4-methylpyridine; 3-ampy = 3-aminopyridine, have been synthesised and studied from the magnetostructural point of view. Compounds **1** and **2** are one-dimensional compounds which show  $[\text{Mn}(\mu_{1,1}\text{-N}_3)_2\text{Mn}]^{2+}$  dimeric entities linked to the two neighbours by **one** end-to-end azido bridge, leading to alternate ferro–antiferromagnetic monodimensional manganese(II) azido compounds. Compounds **1** and **2** are bulk antiferromagnetically coupled systems. The best fit superexchange parameters are:  $J_1 = 3.3(1) \text{ cm}^{-1}$ ,  $J_2 = -5.16(1) \text{ cm}^{-1}$ ,  $g = 2.00(1)$  for **1** and  $J_1 = 2.3(2) \text{ cm}^{-1}$ ,  $J_2 = -6.01(3) \text{ cm}^{-1}$ ,  $g = 2.07(1)$  for **2**.

## Introduction

The chemistry of the manganese(II)–L–azido bridged system, L = N-aromatic ligands, affords high dimensional compounds<sup>1–15</sup> in which the co-ordination mode of the azido bridge may be only  $\mu_{1,3}\text{-N}_3$  (end-to-end, EE), only  $\mu_{1,1}\text{-N}_3$  (end-on, EO) or often alternating 1-D or 2-D systems in which the two kinds of co-ordination modes are found together in the same compound. Correlation has not been found between the properties of the ligand L and the co-ordination mode of the azido bridge, and from the synthetic point of view, the manganese(II)–L–azido system shows unpredictable behaviour, analogous to that observed for copper(II) or nickel(II) azido bridged polynuclear systems. We have described recently the monodimensional alternating compounds  $[\text{Mn}_2(3\text{-Et},4\text{-Mepy})_4(\mu_{1,1}\text{-N}_3)_2(\mu_{1,3}\text{-N}_3)_2]_n$ <sup>11</sup> and  $[\text{Mn}_2(3\text{-bzpy})_4(\mu_{1,1}\text{-N}_3)_2(\mu_{1,3}\text{-N}_3)_2]_n$ ,<sup>12</sup> (3-bzpy = 3-benzoylpyridine) in which the manganese atoms are bridged alternately by **two** end-to-end and **two** end-on azido ligands. Following our research on high-dimensional manganese(II)–(L)–azido bridged systems we now present two new 1-D compounds of the pyridine series, using L = 3-ethyl-4-methylpyridine and 3-aminopyridine to obtain the monodimensional compounds  $[\{\text{Mn}_2(3\text{-Et},4\text{-Mepy})_6(\mu_{1,1}\text{-N}_3)_2(\mu_{1,3}\text{-N}_3)\}_n][\text{PF}_6]_n$  **1** and  $[\{\text{Mn}_2(3\text{-ampy})_4(\mu_{1,1}\text{-N}_3)_2(\mu_{1,3}\text{-N}_3)(\text{N}_3)(\text{H}_2\text{O})\cdot 4\text{H}_2\text{O}\}_n]$  **2**. Compounds **1** and **2** are the first examples, with manganese(II) as the central atom, of one-dimensional compounds with alternating double end-on/single end-to-end azido bridges, giving a ferro–antiferromagnetic (F/AF) alternating system. This structural pattern has been found previously in the Ni(II) compound  $[\text{Ni}_2(\text{Medien})_2(\mu_{1,1}\text{-N}_3)_2(\mu_{1,3}\text{-N}_3)]_n(\text{ClO}_4)_n$ ,<sup>16</sup> [Medien = bis(2-aminoethyl)methylamine] which also presents F/AF alternance. The experimental magnetic susceptibility vs. T data for **1** and **2** have been fitted by using the equation published<sup>8</sup> by Cortés *et al.* for  $S = 5/2$  alternating F/AF coupled 1-D systems, giving the best fit superexchange parameters:  $J_1 = 3.3(1) \text{ cm}^{-1}$  and  $J_2 = -5.16(1) \text{ cm}^{-1}$  for **1** and  $J_1 = 2.3(2) \text{ cm}^{-1}$  and  $J_2 = -6.01(3) \text{ cm}^{-1}$  for **2**.

## Experimental

### Preparation of $[\{\text{Mn}_2(3\text{-Et},4\text{-Mepy})_6(\mu_{1,1}\text{-N}_3)_2(\mu_{1,3}\text{-N}_3)\}_n][\text{PF}_6]_n$ **1**

Compound **1** was synthesised by mixing an aqueous-ethanolic solution (1:1, 50 ml) of manganese nitrate tetrahydrate (1.00 g, 4 mmol) and potassium hexafluorophosphate (0.80 g, 4.3 mmol) and (1.10 g, 9 mmol) of 3-ethyl-4-methylpyridine dissolved in 20 ml of ethanol, followed by dropwise addition of a concentrated aqueous solution of sodium azide (0.65 g, 10 mmol). The clear solution was left to stand in the dark for several days. Green crystals suitable for X-ray determination were formed. Yield: 65%. Analytical data: found % (calc. for  $\text{Mn}_2\text{C}_{48}\text{H}_{66}\text{N}_{15}\text{PF}_6$  %): C, 51.9(52.0); H, 5.9(6.0); N, 19.1(19.0); Mn, 9.8(9.9). IR spectra: compound **1** shows two very strong split bands assigned for the asymmetric stretching vibrations ( $\nu_{\text{as}} \text{N}_3$ ) centred at 2055 vs and 2110 vs  $\text{cm}^{-1}$ . No band could be attributed to the ( $\nu_{\text{s}} \text{N}_3$ ) mode in the 1280–1360  $\text{cm}^{-1}$  region.

### Preparation of $[\{\text{Mn}_2(3\text{-ampy})_4(\mu_{1,1}\text{-N}_3)_2(\mu_{1,3}\text{-N}_3)(\text{N}_3)(\text{H}_2\text{O})\cdot 4\text{H}_2\text{O}\}_n]$ **2**

Compound **2** was synthesised by mixing an aqueous solution (30 ml) of manganese perchlorate hexahydrate (1.50 g, 4.1 mmol) and 3-aminopyridine (1.00 g, 10.6 mmol) dissolved in 10 ml of methanol, followed by dropwise addition of a saturated aqueous solution of sodium azide (0.65 g, 10 mmol). The final solution was filtered off after 24 hours and then left to stand in the dark for several weeks. Yellow crystals suitable for X-ray determination were formed. Yield: 60%. Analytical data; found % (calc. for  $\text{Mn}_2\text{C}_{20}\text{H}_{34}\text{N}_{20}\text{O}_5$  %): C, 32.4(32.3); H, 4.4(4.6); N, 37.5(37.6); Mn, 14.7(14.8). IR spectra: in the 2000–2150  $\text{cm}^{-1}$  region the complex shows three very strong split bands assigned to the asymmetric stretching vibrations ( $\nu_{\text{as}} \text{N}_3$ ) centred at 2088 vs, 2058 vs and 2035 vs  $\text{cm}^{-1}$ . In the 1280–1360  $\text{cm}^{-1}$  region a moderate shoulder at 1298  $\text{cm}^{-1}$  could be attributed to the  $\nu_{\text{s}} \text{N}_3$  mode.

**Table 1** Crystal data and structure refinement for  $[\{\text{Mn}_2(3\text{-Et}, 4\text{-Mepy})_6(\mu_{1,1}\text{-N}_3)_2(\mu_{1,3}\text{-N}_3)\}_n][\text{PF}_6]_n$  **1** and  $[\{\text{Mn}_2(3\text{-ampy})_4(\mu_{1,1}\text{-N}_3)_2(\mu_{1,3}\text{-N}_3)(\text{N}_3)(\text{H}_2\text{O})\cdot 4\text{H}_2\text{O}\}_n]$  **2**

	<b>1</b>	<b>2</b>
Formula	$\text{C}_{48}\text{H}_{66}\text{F}_6\text{Mn}_2\text{N}_{15}\text{P}$	$\text{C}_{20}\text{H}_{34}\text{Mn}_2\text{N}_{20}\text{O}_5$
Formula weight	1108.01	744.56
Space group	$P\bar{1}$	$C2/c$
$a/\text{\AA}$	8.988(3)	16.881(6)
$b/\text{\AA}$	10.924(4)	12.913(3)
$c/\text{\AA}$	15.272(5)	15.741(5)
$\alpha^\circ$	99.50(3)	—
$\beta^\circ$	106.81(3)	106.87(2)
$\gamma^\circ$	98.56(3)	—
$V/\text{\AA}^3$	1384.7(8)	3287.6(17)
$Z$	1	4
$T/\text{K}$	25(2)	25(2)
$\lambda(\text{Mo-K}\alpha)/\text{\AA}$	0.71069	0.71069
$D_{\text{calc}}/\text{g cm}^{-3}$	1.329	1.504
$\mu(\text{Mo-K}\alpha)/\text{mm}^{-1}$	0.552	0.833
$R^a$	0.0881	0.0373
$R^2_w{}^b$	0.2222 <sup>b</sup>	0.0782 <sup>b</sup>

<sup>a</sup>  $R(F_o) = \sum ||F_o| - |F_c|| / \sum |F_o|$ . <sup>b</sup>  $R_w(F_o) = \{ \sum [w((F_o)^2 - (F_c)^2)^2] / \sum [w((F_o)^2)] \}^{1/2}$ .

### Spectral and magnetic measurements

Infrared spectra (4000–400  $\text{cm}^{-1}$ ) were recorded from KBr pellets on a Perkin-Elmer 380-B spectrophotometer. Magnetic susceptibility measurements were carried out for **1** on polycrystalline samples with a SQUID apparatus working in the range 2–300 K under magnetic fields of approximately 0.1 T. Magnetic measurements were carried out for **2** with a Faraday type magnetometer (MANICS DSM8) equipped with an Oxford CF 1200 S helium continuous-flow cryostat working in the temperature range 4–300 K. Diamagnetic corrections were estimated from Pascal Tables. EPR spectra were recorded with a Bruker ES200 spectrometer at X-band frequency.

### Crystallographic data collection and refinement

The X-ray single-crystal data for both compounds were collected on a modified STOE four-circle diffractometer. The crystallographic data, the conditions for the intensity data collection and some features of the structure refinements are listed in Table 1. Additional corrections for intensity decay, and for absorption using the DIFABS<sup>17</sup> computer program, were applied for data processing. The structures were solved by direct methods using the SHELXS-86<sup>18</sup> computer program, and refined by full-matrix least-squares methods on  $F^2$ , using the SHELXL-93<sup>19</sup> program incorporated in the SHELXTL/PC V 5.03<sup>20</sup> program library and the graphics program PLUTON.<sup>21</sup> Partial disorder with a split occupancy of 0.50 was observed for the azido group N(31)–N(32)–N(33), and water molecules O(2), O(3) and O(4) in **2**, and also for two of the substituted pyridine molecules and the  $\text{PF}_6^-$  counter anion in **1**. The hydrogen atoms bonded to carbon atoms of pyridine derivative ligands were located on calculated positions by the use of the HFIX utility of the SHELXL-93 program; the remaining hydrogen positions of **2** were located from difference maps and included in final refinement cycles by the use of N–H and O–H distance restraints. Significant bond parameters for **1** and **2** are given in Tables 2 and 3.

CCDC reference number 186/1749.

See <http://www.rsc.org/suppdata/ft/a9/a907835e/> for crystallographic files in .cif format.

## Results and discussion

### Synthesis

The large number of polynuclear Mn(II)-azide compounds

**Table 2** Selected bond lengths ( $\text{\AA}$ ) and angles ( $^\circ$ ) for  $[\{\text{Mn}_2(3\text{-Et}, 4\text{-Mepy})_6(\mu_{1,1}\text{-N}_3)_2(\mu_{1,3}\text{-N}_3)\}_n][\text{PF}_6]_n$  **1**

Mn(1)···Mn(1A)	3.459(2)	Mn(1)···Mn(1B)	6.455(3)
Mn(1)–N(11)	2.164(6)	Mn(1)–N(21A)	2.207(5)
Mn(1)–N(21)	2.262(6)	Mn(1)–N(2)	2.28(3)
Mn(1)–N(1)	2.294(6)	Mn(1)–N(3)	2.290(6)
N(12)–N(11B)	1.163(6)	N(11)–N(12)	1.163(6)
N(21)–Mn(1A)	2.207(5)	N(21)–N(22)	1.200(7)
		N(22)–N(23)	1.152(8)
N(11)–Mn(1)–N(21A)	169.8(2)	N(11)–Mn(1)–N(21)	91.4(2)
N(21A)–Mn(1)–N(21)	78.6(2)	N(11)–Mn(1)–N(2)	90.4(6)
N(21A)–Mn(1)–N(2)	89.6(5)	N(21)–Mn(1)–N(2)	98.3(6)
N(21A)–Mn(1)–N(3)	89.9(2)	N(11)–Mn(1)–N(3)	91.5(3)
N(2)–Mn(1)–N(3)	171.6(6)	N(21)–Mn(1)–N(3)	89.8(2)
N(11)–Mn(1)–N(1)	94.2(2)	N(32)–Mn(1)–N(3)	175.7(5)
N(21)–Mn(1)–N(1)	174.4(2)	N(21A)–Mn(1)–N(1)	95.8(2)
N(32)–Mn(1)–N(1)	88.6(6)	N(2)–Mn(1)–N(1)	81.8(6)
N(12)–N(11)–Mn(1)	150.5(5)	N(3)–Mn(1)–N(1)	89.9(2)
N(22)–N(21)–Mn(1A)	131.6(5)	N(11)–N(12)–N(11B)	180.0
Mn(1A)–N(21)–Mn(1)	101.4(2)	N(22)–N(21)–Mn(1)	118.5(4)
		N(23)–N(22)–N(21)	179.1(7)

Symmetry codes: (A)  $-x, -y + 1, -z + 2$ ; (B)  $-x + 1, -y + 1, -z + 2$ .

**Table 3** Selected bond lengths ( $\text{\AA}$ ) and angles ( $^\circ$ ) for  $[\{\text{Mn}_2(3\text{-ampy})_4(\mu_{1,1}\text{-N}_3)_2(\mu_{1,3}\text{-N}_3)(\text{N}_3)(\text{H}_2\text{O})\cdot 4\text{H}_2\text{O}\}_n]$  **2**

Mn(1)···Mn(1A)	3.4327(13)	Mn(1)···Mn(1B)	6.169(2)
Mn(1)–N(21)	2.188(2)	Mn(1)–O(3)	2.187(5)
Mn(1)–N(11)	2.214(2)	Mn(1)–N(31)	2.243(4)
Mn(1)–N(3)	2.254(2)	Mn(1)–N(1)	2.272(2)
Mn(1)–N(11A)	2.280(2)	N(11)–N(12)	1.181(2)
N(12)–N(13)	1.148(3)	N(21)–N(22)	1.164(2)
N(22)–N(21B)	1.164(2)	N(31)–N(32)	1.179(5)
N(32)–N(33)	1.131(6)		
N(21)–Mn(1)–O(3)	91.78(14)	N(21)–Mn(1)–N(11)	169.70(7)
O(3)–Mn(1)–N(11)	98.52(14)	N(21)–Mn(1)–N(31)	86.92(11)
N(11)–Mn(1)–N(31)	103.37(10)	N(21)–Mn(1)–N(3)	90.51(6)
O(3)–Mn(1)–N(3)	87.61(13)	N(11)–Mn(1)–N(3)	90.41(6)
N(31)–Mn(1)–N(3)	87.91(9)	N(21)–Mn(1)–N(1)	90.39(7)
O(3)–Mn(1)–N(1)	88.30(13)	N(11)–Mn(1)–N(1)	89.43(6)
N(31)–Mn(1)–N(1)	88.08(9)	N(3)–Mn(1)–N(1)	175.84(6)
N(21)–Mn(1)–N(11A)	89.31(7)	O(3)–Mn(1)–N(11A)	178.91(13)
N(11)–Mn(1)–N(11A)	80.40(6)	N(31)–Mn(1)–N(11A)	176.22(10)
N(3)–Mn(1)–N(11A)	92.35(6)	N(1)–Mn(1)–N(11A)	91.73(6)
N(12)–N(11)–Mn(1)	132.47(14)	N(12)–N(11)–Mn(1A)	123.52(14)
Mn(1)–N(11)–Mn(1A)	99.60(6)	O(3)–N(12)–N(11)	178.9(2)
N(22)–N(21)–Mn(1)	133.07(12)	N(21B)–N(22)–N(21)	180.0
N(32)–N(31)–Mn(1)	117.3(3)	N(33)–N(32)–N(31)	172.0(5)

Symmetry codes: (A)  $-x, -y, -z + 1$ ; (B)  $-x, y, -z + 1/2$ .

reported to date may be classified in two main groups: one corresponds to the  $\text{Cat}[\text{Mn}(\text{N}_3)_3]$  formula, in which the variation of the cation  $\text{Cat} = \text{Cs}^+, \text{N}(\text{Me})_4^+, \text{N}(\text{Et})_4^+$  affords different topologies in three-dimensional systems or unexpected double Mn<sup>II</sup> chains.<sup>14,15</sup> The second kind of compounds, with general formula  $[\text{Mn}(\text{L})_2(\text{N}_3)_2]$ , correspond to neutral systems with a variety of dimensionalities and topologies.<sup>1–13</sup> In this latter kind of compound the similar ability of the azido ligand to coordinate in the end-to-end or end-on modes makes unpredictable, *a priori*, the topology of the resulting compound. In most of the cases packing forces or  $\pi$ – $\pi$  interactions between the aromatic rings seem the determinant factors. In this work we show the first example of a potential new series of compounds with general formula  $[\text{Mn}_2(\text{L})_6(\text{N}_3)_3]\text{A}$ ,  $[\{\text{Mn}_2(3\text{-Et}, 4\text{-Mepy})_6(\mu_{1,1}\text{-N}_3)_2(\mu_{1,3}\text{-N}_3)\}_n][\text{PF}_6]_n$  **1**, which present also a new topology for Mn(II)–L–azido compounds: alternating double end-on/single end-to-end azido bridges, giving a ferro–antiferromagnetic (F/AF) alternating system. With regard to the unpredictable behaviour of the manganese(II)–L–azido system, we have previously obtained, with the same L ligand the

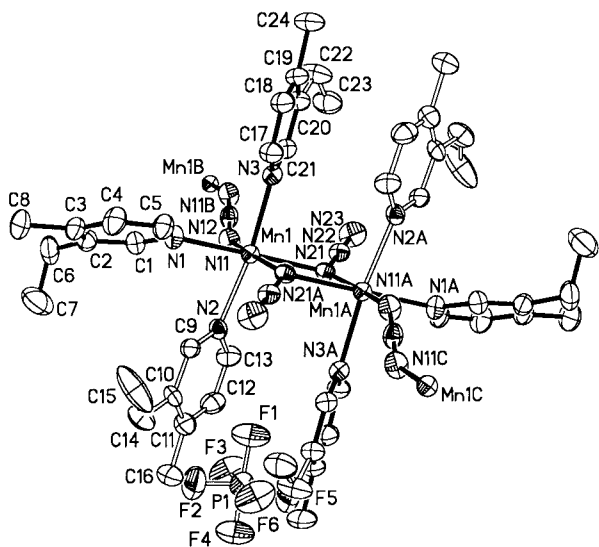


**Fig. 1**  $[\{\text{Mn}_2(3\text{-Et},4\text{-Mepy})_6(\mu_{1,1}\text{-N}_3)_2(\mu_{1,3}\text{-N}_3)\}_n][\text{PF}_6]_n$  **1**: ORTEP<sup>22</sup> view (30% probability) of dimeric subunit. Only one orientation of disordered parts (with half occupancy as indicated by open stick bonds) is given for clarity. Hydrogen atoms are omitted.

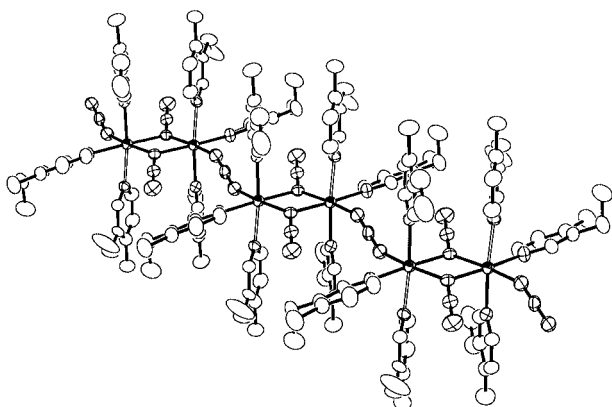


**Fig. 3**  $[\{\text{Mn}_2(3\text{-ampy})_4(\mu_{1,1}\text{-N}_3)_2(\mu_{1,3}\text{-N}_3)(\text{N}_3)(\text{H}_2\text{O})\cdot 4\text{H}_2\text{O}\}_n]$  **2**: ORTEP view (40% probability) of a dimeric subunit. Hydrogen atoms are omitted. Disordered ligands with half occupancy are indicated by open stick bonds. Note: O(3A) and N(31)–N(32)–N(33) and lattice water molecules O(1), O(2) and O(4) are also omitted for clarity.

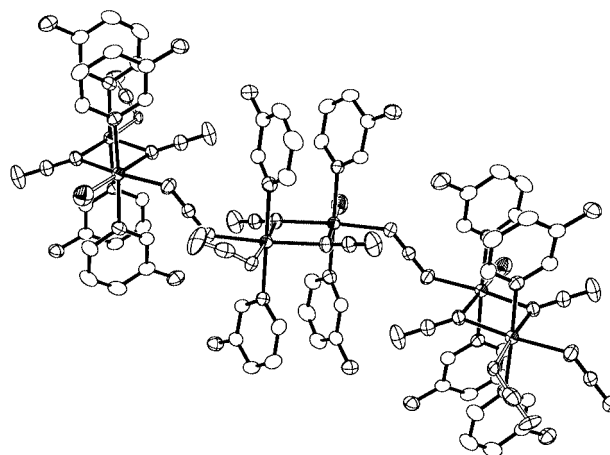


**Fig. 2** Sequence of the bridging azido ligands in the polymeric  $[\text{Mn}_2(3\text{-Et},4\text{-Mepy})_6(\mu_{1,1}\text{-N}_3)_2(\mu_{1,3}\text{-N}_3)]_n^{++}$  cation of **1**. The chains of polyhedra are oriented along the *a*-axis of the unit cell.

**Fig. 4** Sequence of the bridging azido ligands in the neutral  $[\text{Mn}_2(3\text{-ampy})_4(\mu_{1,1}\text{-N}_3)_2(\mu_{1,3}\text{-N}_3)(\text{N}_3)(\text{H}_2\text{O})]_n$  chain of **2**. The 1-D system is oriented along the *c*-axis of the unit cell.

compound  $[\text{Mn}_2(3\text{-Et},4\text{-Mepy})_4(\mu_{1,1}\text{-N}_3)_2(\mu_{1,3}\text{-N}_3)_2]_n^{11}$  an F/AF alternating chain in which the manganese atoms are bridged alternately by **two** end-to-end and **two** end-on azido ligands, by mixing  $\text{Mn}(\text{ClO}_4)_2\cdot 6\text{H}_2\text{O}$ , 3-Et,4-Mepy and  $\text{NaN}_3$ . This unpredictable behaviour appears newly for the 3-ampy ligand and the perchlorate anion, compound **2**, which results in a neutral compound with the same bridging skeleton as **1** but with general formula  $[\text{Mn}(\text{L})_2(\text{N}_3)_2]$ .

### Crystal structures

$[\{\text{Mn}_2(3\text{-Et},4\text{-Mepy})_6(\mu_{1,1}\text{-N}_3)_2(\mu_{1,3}\text{-N}_3)\}_n][\text{PF}_6]_n$  **1**. The labelled diagram for **1** is shown in Fig. 1. A chain perspective of the same compound is shown in Fig. 2. The structure consists of octahedrally co-ordinated manganese atoms in which the co-ordination sites are occupied by three 3-ethyl-4-methylpyridine ligands in *mer* arrangement and three bridging azido ligands. Two azide groups act as end-on bridging ligands forming dimeric subunits. These dimeric subunits are further linked by end-to-end bridging azido ligands, thus giving a monodimensional system with alternating single  $\mu_{1,3}$  and double  $\mu_{1,1}$  bridges along the *a*-axis of the unit cell (Fig. 2). Inversion centres are placed in the dimeric subunits and in the end-to-end bridges. The bond parameters related with the end-on bridges are  $\text{Mn}(1)\text{--N}(21) = 2.262(6)$  Å,  $\text{Mn}(1)\text{--N}(21\text{A}) = 2.207(5)$  Å,  $\text{Mn}(1)\text{--N}(21)\text{--Mn}(1\text{A}) = 101.4(2)^\circ$  and the bond parameters related to the end-to-end bridges are  $\text{Mn}(1)\text{--N}(11) = 2.164(6)$

Å,  $\text{Mn}(1)\text{--N}(11)\text{--N}(12) = 150.5(5)^\circ$ . The  $\text{Mn}(1)\cdots\text{Mn}(1\text{A})$  distance is  $3.459(2)$  Å and the  $\text{Mn}(1)\cdots\text{Mn}(1\text{B})$  distance  $6.455(3)$  Å. The  $\text{Mn}(1)\text{--N}(11)\text{--N}(12)\text{--N}(11\text{B})\text{--Mn}(1\text{B})$  torsion angle is  $180.0(2)^\circ$ . The positive charged chains of (**1**) are well isolated by the 3-Et,4-Mepy-ligands and the  $\text{PF}_6^-$  counter anions. The minimum Mn–Mn interchain distance is  $10.004(4)$  Å.

$[\{\text{Mn}_2(3\text{-ampy})_4(\mu_{1,1}\text{-N}_3)_2(\mu_{1,3}\text{-N}_3)(\text{N}_3)(\text{H}_2\text{O})\cdot 4\text{H}_2\text{O}\}_n]$  **2**. The labelled diagram for **2** is shown in Fig. 3. A chain perspective of the same compound is shown in Fig. 4. The structure consists of octahedrally co-ordinated manganese atoms in which the co-ordination sites are occupied by three bridging azido ligands in *mer* arrangement, two *trans* 3-aminopyridine ligands and one terminal azido ligand or aqua ligand (these ligands are disordered with half occupancy; the separation of split positions of N(31) and O(3) is  $0.20$  Å). One azido acts as an end-to-end bridging ligand with one neighbouring manganese atom and the other two act as end-on bridging ligands with another neighbouring manganese atom, giving a monodimensional system with alternating single end-to-end and double end-on bridges along the *c*-axis of the unit cell (Fig. 4). The bond parameters related to the end-on bridges are  $\text{Mn}(1)\text{--N}(11) = 2.214(2)$  Å,  $\text{Mn}(1)\text{--N}(11\text{A}) = 2.280(2)$  Å,  $\text{Mn}(1)\text{--N}(11)\text{--Mn}(1\text{A}) = 99.60(6)^\circ$  and the bond parameters related to the end-to-end bridges are  $\text{Mn}(1)\text{--N}(21) = 2.188(2)$  Å,  $\text{Mn}(1)\text{--}$

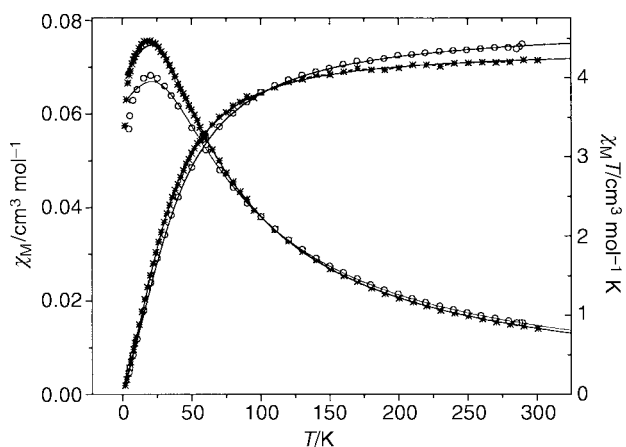


Fig. 5 Molar magnetic susceptibility vs.  $T$  and  $\chi_M T$  vs.  $T$  plots for **1** (\*) and **2** (○). Solid lines show the best fit obtained for **1** and **2**.

$N(21)-N(22) = 133.1(1)^\circ$ .  $Mn(1) \cdots Mn(1B) = 6.169(2)$  Å and  $Mn(1) \cdots Mn(1A) = 3.433(1)$  Å. The torsion angle  $Mn(1)-N(21)-N(21B)-Mn(1B)$  is  $156.1(1)^\circ$ . The neutral chains of **2** are well isolated by the ligands and lattice water molecules, the minimum Mn–Mn interchain distance being  $8.596(3)$  Å.

### Magnetic properties

The  $\chi_M T$  product and the molar magnetic susceptibilities vs.  $T$  in the 300–4 K range of **1** and **2** are plotted in Fig. 5. The overall behaviour of **1** and **2** corresponds to a bulk antiferromagnetically coupled system. For **1**  $\chi_M T$  decreases on cooling from  $4.22 \text{ cm}^3 \text{ K mol}^{-1}$  at 300 K and tends to zero at low temperature whereas the  $\chi_M$  vs.  $T$  plot increases on cooling from  $1.40 \times 10^{-2} \text{ cm}^3 \text{ mol}^{-1}$  at 300 K and has a maximum of  $7.6 \times 10^{-2} \text{ cm}^3 \text{ mol}^{-1}$  at 20 K, after which it decreases. For **2**  $\chi_M T$  decreases on cooling from  $4.43 \text{ cm}^3 \text{ K mol}^{-1}$  at 290 K and tends to zero at low temperature and the  $\chi_M$  vs.  $T$  plot increases on cooling from  $1.53 \times 10^{-2} \text{ cm}^3 \text{ mol}^{-1}$  at 290 K and has a maximum of  $6.8 \times 10^{-2} \text{ cm}^3 \text{ mol}^{-1}$  at 21 K, after which it decreases.

The magnetic data of **1** and **2**, according with their structures, were analysed by means of the expression recently published<sup>8</sup> by Cortés *et al.* for alternating ferro–antiferro monodimensional  $S = 5/2$  compounds derived from the spin Hamiltonian  $H = -J_1 \sum S_{2i} S_{2i+1} - J_2 \sum S_{2i+1} S_{2i+2}$ . Best fit parameters were  $J_1 = 3.3(1) \text{ cm}^{-1}$ ,  $J_2 = -5.16(1) \text{ cm}^{-1}$  and  $g = 2.00(1)$ , for **1** and  $J_1 = 2.3(2) \text{ cm}^{-1}$ ,  $J_2 = -6.01(3) \text{ cm}^{-1}$  and  $g = 2.07(1)$  for **2**.  $J_1$  and  $J_2$  correspond to the double EO and to the single EE superexchange pathways respectively. The similar antiferromagnetic  $J$  values for **1** ( $-5.16(1) \text{ cm}^{-1}$ ) and **2** ( $-6.01(3) \text{ cm}^{-1}$ ) can be explained according to the model previously described by us:<sup>2</sup> the plot of  $\Sigma \Delta^2$  vs. the Mn–N–N(azido) angle (fixing the Mn–N–N–N–Mn torsion angle at  $180^\circ$ ) shows a maximum of  $J_{AF}$  for low Mn–N–N bond angles close to  $110^\circ$  and a minimum for large Mn–N–N angles, close to  $160^\circ$ . On the other hand, the study of the torsion angles shows that the AF interaction should be maximum for the planar arrangement of the manganese ions and the azido bridge and should be minimum for high torsion values. With the first criterion,  $J_{AF}$  for **2** ( $Mn(1)-N(21)-N(22) = 133.1^\circ$ ) should be greater than  $J_{AF}$  for **1** ( $Mn(1)-N(11)-N(12) = 150.5^\circ$ ) but the Mn–N–N–Mn torsion angles of **2** and **1** are  $156.1^\circ$  and  $180.0^\circ$  respectively

and this second effect compensates the different Mn–N–N angles.

### EPR Spectra

EPR spectra recorded on powdered samples at room temperature show a sharp isotropic signal centred at  $g = 2.00$  (peak-to-peak line width 132 G) for **1** and also a sharp isotropic signal centred at  $g = 2.00$  (peak-to-peak line width 55 G) for **2**.

### Acknowledgements

This research was partially supported by CICYT (Grant PB96/0163) and OENB (grants 6630 and 7967). F. A. M. thanks Prof. C. Kratky and Dr Belaj (University of Graz) for use of experimental equipment.

### References

- 1 M. A. S. Goher and F. A. Mautner, *Croat. Chem. Acta*, 1990, **63**, 559.
- 2 A. Escuer, R. Vicente, M. A. S. Goher and F. A. Mautner, *Inorg. Chem.*, 1996, **35**, 6386.
- 3 G. De Munno, M. Julve, G. Viau, F. Lloret, J. Faus and D. Viterbo, *Angew. Chem., Int. Ed. Engl.*, 1996, **35**, 1807.
- 4 R. Cortés, L. Lezama, J. L. Pizarro, M. I. Arriortua and T. Rojo, *Angew. Chem., Int. Ed. Engl.*, 1996, **35**, 1810.
- 5 A. Escuer, R. Vicente, F. A. Mautner and M. A. S. Goher, *Inorg. Chem.*, 1997, **36**, 3440.
- 6 A. Escuer, R. Vicente, M. A. S. Goher and F. A. Mautner, *Inorg. Chem.*, 1995, **34**, 5707.
- 7 A. Escuer, R. Vicente, M. A. S. Goher and F. A. Mautner, *J. Chem. Soc., Dalton Trans.*, 1997, 4431.
- 8 R. Cortés, M. Drillon, X. Solans, L. Lezama and T. Rojo, *Inorg. Chem.*, 1997, **36**, 677.
- 9 A. Escuer, R. Vicente, M. A. S. Goher and F. A. Mautner, *Inorg. Chem.*, 1998, **37**, 782.
- 10 H.-Y. Shen, D.-Z. Liao, Z.-H. Jiang, S.-P. Yan, B.-W. Sun, G.-L. Wang, X.-K. Yao and H. G. Wang, *Chem. Lett.*, 1998, 469.
- 11 M. A. M. Abu-Youssef, A. Escuer, M. A. S. Goher, F. A. Mautner and R. Vicente, *Eur. J. Inorg. Chem.*, 1999, 687.
- 12 M. A. M. Abu-Youssef, A. Escuer, D. Gatteschi, M. A. S. Goher, F. A. Mautner and R. Vicente, *Inorg. Chem.*, 1999, **38**, 5716.
- 13 J. L. Manson, A. M. Arif and J. S. Miller, *Chem. Commun.*, 1999, 1479.
- 14 M. A. S. Goher, J. Cano, Y. Journaux, M. A. M. Abu-Youssef, F. A. Mautner, A. Escuer and R. Vicente, *Chem. Eur. J.*, accepted for publication.
- 15 F. A. Mautner, R. Cortés, L. Lezama and T. Rojo, *Angew. Chem., Int. Ed. Engl.*, 1996, **35**, 78.
- 16 A. Escuer, R. Vicente, M. S. El Fallah, S. B. Kumar, F. A. Mautner and D. Gatteschi, *J. Chem. Soc., Dalton Trans.*, 1998, 3905.
- 17 N. Walker and D. Stuart, *Acta Crystallogr., Sect. A*, 1983, **39**, 158.
- 18 G. M. Sheldrick, SHELXS-86, Program for the Solution of Crystal Structure, University of Göttingen, Germany, 1986.
- 19 G. M. Sheldrick, SHELXL-93, Program for the Refinement of Crystal Structure, University of Göttingen, Germany, 1993.
- 20 SHELXTL 5.03 (PC-Version), Program library for the Solution and Molecular Graphics, Siemens Analytical Instruments Division, Madison, WI, 1995.
- 21 A. L. Spek, PLUTON-92, University of Utrecht, 3584, CH Utrecht, The Netherlands, 1992.
- 22 C. K. Johnson, ORTEP, Report ORNL-5138, Oak Ridge National Laboratory, Oak Ridge, TN, 1976.

Paper a907835e